DOI: 10.21062/mft.2021.053 http://www.journalmt.com

Comparison on Milling Force Model Prediction of New Cold Saw Blade Milling Cutter Based on Deep Neural Network and Regression Analysis

Shuailiang Guo (0000-0003-4146-5616)[1], Han Zheng (0000-0002-2076-9269)[2], Xiangzeng Liu (0000-0002-2751-6096)[2], Lizhi Gu (0000-0002-0382-4959)[1]
[1]College of Mechanical Engineering and Automation, National Huaqiao University, Xiamen, 361021. China. Email: guoshuailiang01@126.com; gulizhi888@163.com
[2]School of Computer Science and Technology at Xidian University, Xi'an, 710071. China. Email: zhenghanhqu@163.com; xzliu@xidian.edu.cn

A four factors and three levels orthogonal milling force (MF) test is designed, which qualitatively obtains the influence of four factors, namely workpiece material, workpiece diameter, milling speed and feed per tooth, on MF of the new cold saw blade milling cutter (NCSBMC), then further verifies the reliability of test data with simulation analysis of MF. The multiple linear regression analysis and deep neural network (DNN) are used to accurately fit and predict the magnitude of MF in three directions of NCSBMC, taking into account the influence of workpiece material factors on MF. Compared with the results of empirical formula, DNN has higher prediction accuracy. The research results provide theoretical guidance for the optimization of milling parameters in actual machining process.

Keywords: NCSBMC, MF, Orthogonal Test, Multiple Linear Regression Analysis, DNN

1 Introduction

Compared with the traditional hot saw blade milling cutter (THSBMC), NCSBMC has the advantages of high sizing accuracy, high productivity and good quality workpiece cross-section [1]. Therefore, it is widely used in the machining of various profiles, pipes and solid bar materials [2]. The teeth of NCSBMC are made of Ti(C,N)-based metal-ceramic material, their hardness can reach about 92 HRC, which is higher than the hardness of high-speed steel saw blade milling cutter of 60-70 HRC and carbide saw blade milling cutter of 76-82 HRC. During milling process, NCSBMC exhibits lower temperature, lower speed, larger feed and higher saw removal rate than others [3], so it has important academic significance and engineering application value for MF study of NCSBMC.

At present, MF model prediction mainly includes analytical method, empirical formula method and neural network method, each of which has its own limitations. Due to certain limitations in study of milling mechanism, individual physical parameters in milling process are difficult to accurately obtain, so it is difficult to accurately describe milling process using mathematical models, which seriously affects the prediction accuracy of analytical model [4]. The establishment of empirical formulas relies on large amounts of accurate experimental data, incidental measurement errors and experimental errors will have a great impact on establishment empirical formulas. In addition, empirical formulas rarely consider the influence of material characteristics on MF. Although the prediction accuracy of DNN model depends on training samples, DNN model itself has the characteristics of self-adaptation, self-organization, self-learning, nonlinear mapping, fault tolerance and correction capabilities, and high-speed parallel computing capabilities [5]. Since there is a high nonlinear relationship among milling parameters, workpiece material and MF, and DNN is very powerful in nonlinear modeling [6], the use of DNN model to predict MF has obvious advantage.

In traditional MF research area, S. Campocasso et al [7] performed the same heat treatment and mechanical performance treatment on specific five processing materials, and obtained the correlation coefficient between mechanical performance and cutting force through cutting experiments and mechanical performance comparison analysis. János Kundrák et al [8] studied the effect of feed on the MF and chip size ratio of face milling at different milling speeds. Geng et al [9] studied the effect of milling speed, feed per tooth and radial depth on the MF by simulating the milling of GH4169 nickel base superalloy with finite element software. Li et al [10] measured the force and net power of the saw blade during sawing process and obtained the distribution of sawing force within the sawing arc zone by studying the location of the point of action of the combined sawing force. Hu et al [11] reviewed the cutting force modeling method to provide a theoretical basis for cutting simulation research. Tang et al [12] calculated and studied the force and cutting power of the saw blade during cold sawing,

and Zhu et al [13] established a transient mechanical model that can accurately describe the cut in and cut out of each tooth of the milling cutter, and concluded that the axial force can be apply to predict the wear of milling cutter. S. Turchetta and L. Sorrentino [14] used a CNC machining center to study the effect of changing machining parameters on stone cutting.

Due to the rapid development of artificial intelligence, scholars and experts have introduced neural networks to study MF. Kais I. Abdul-lateef Al-Abdullah et al [15] accorded to the experimental data of artificial tissue milling with bone milling cutter, the corresponding force and temperature models were established by using artificial neural network (ANN). Li et al [16] used a neural network model to predict tool wear and cutting force, this work concluded that the neural network model is able to consider more influential factors in the machining process and has a higher prediction accuracy than the empirical formula. Wang et al [17] established a "transfer network" model for cutting force prediction based on the simulation results. Compared with the neural network model based on experimental samples, the transfer network has better performance in the case of sufficient data. However, migration learning research is currently immature and it is difficult to choose among the available training models for the particular task at hand. Ali Yeganefar et al [18] studied the prediction and optimization of surface roughness and cutting force in aluminum alloy milling operations using four methods, and this paper concluded that the neural network had higher prediction accuracy compared to support vector regression and regression analysis. The literature [15-18] showed that neural network models are very effective in predicting MF and neural network has great potential for application and development in the field of machining.

According to the literature review, we can know that there are few systematic research papers about the effect of workpiece material on MF. In this paper, workpiece material, workpiece diameter, milling speed and feed per tooth are chosen as the input variables to predict MF of NCSBMC based on regression analysis and DNN.

2 Experiment and simulation

2.1 Test platform construction

A four factors and three levels orthogonal test was designed to examine the effect of four factors on the MF of NCSBMC. The metrics are the magnitude of F_X, F_Y and F_Z. The four factors and three levels for orthogonal tests are shown in Tab. 1.

Fig. 1 *Workpiece materials and diameter.*

Tab. 1 *Four factors and three levels orthogonal test*

Factors Levels	Workpiece material(M)	Workpiece diameter (D)(mm)	Milling speed (R)(RPM)	Feed per tooth (W)(mm)
1	45steel	32	96	0.020
2	40Cr	36	110	0.025
3	Q235B	38	115	0.030

A NCSBMC with 60 teeth, tool diameter 460 mm and saw teeth rake angle -9°, rear angle 5.5°, was used to sawing solid round bar under dry condition. MF tests were performed on an intelligent circular sawing machine (EVERSING P-150B, power 15 kW). A three-way dynamometer (Kistler 9257B) with a sampling frequency of 20 KHz was used to obtain the milling forces in Cartesian coordinates in all three axis directions. The workpieces were placed, positioned and clamped in a self-designed fixture, which was fixed to the dynamometer by means of four M8 screws, and the dynamometer was fixed to the test platform. Workpiece materials and MF experimental device are shown in Figs. 1 and 2, respectively.

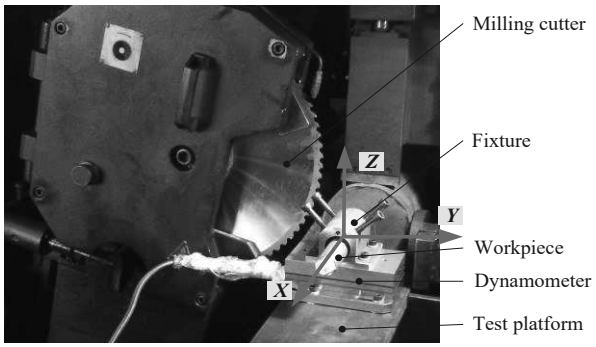

Fig. 2 *MF experimental device*

2.2 Experimental data processing and analysis

L9 (3^4) was chosen to design the MF experiment, and 9 groups of machining were performed, with each group repeated three times, then the three maximum MF obtained for the F_X, F_Y and F_Z in each group were averaged to obtain MF sizes for the F_X, F_Y and F_Z of NCSBMC as shown in Tab. 2.

According to the orthogonal design data processing method, the *K*-values and the mean of the *K*-values were calculated for MF measurement data of NCSBMC, and MF numerical calculation values of NCSBMC are shown in Tab. 3.

Tab. 2 *Experimental values for measuring MF of NCSBMC*

Column / Group	M	D	R	W	Maximum MF (N)		
	1	2	3	4	F_X	F_Y	F_Z
1	45#	32	96	0.020	23.582	161.694	379.150
2	45#	36	110	0.025	24.577	194.348	484.780
3	45#	38	115	0.030	28.768	222.858	547.856
4	40Cr	32	110	0.030	65.111	233.553	467.518
5	40Cr	36	115	0.020	26.531	159.030	367.987
6	40Cr	38	96	0.025	33.011	195.684	474.098
7	Q235	32	115	0.025	37.317	144.701	419.107
8	Q235	36	96	0.030	40.957	182.088	526.890
9	Q235	38	110	0.020	43.558	170.894	424.363

Tab. 3 *Numerical calculation of MF for NCSBMC*

Factors / Indexes	F_X (N)				F_Y (N)				F_Z (N)			
	M	D	R	W	M	D	R	W	M	D	R	W
K_1	77	126	98	94	579	540	540	492	1412	1266	1380	1172
K_2	125	92	133	95	588	536	599	535	1310	1380	1377	1378
K_3	122	105	93	135	498	589	527	639	1370	1446	1335	1542
$\overline{k_1}$	26	42	33	31	193	180	180	164	471	422	460	391
$\overline{k_2}$	42	31	44	32	196	179	200	178	437	460	459	459
$\overline{k_3}$	41	35	31	45	166	197	176	213	457	482	445	514

Plotting the values of $\overline{k_1}$, $\overline{k_2}$ and $\overline{k_3}$ from Tab. 3, we can obtain the relationship between four factors and three indicators, as shown in Fig. 3. In Fig. 3, F_Z is the largest in milling process, followed by F_Y, and F_X is the smallest. Overall, the feed per tooth has obvious influence on MF in three directions. A primary and secondary analysis of the four influencing factors based on the magnitude of F_X, F_Y and F_Z fluctuations, as follows:

The influence on the F_X is as follows: workpiece material > feed per tooth > milling speed > working diameter.

The influence on the F_Y is as follows: feed per tooth > workpiece material > milling speed > working diameter.

The influence on the F_Z is as follows: feed per tooth > workpiece diameter > workpiece material > milling speed.

2.3 Comparative analysis of simulation and experiment

Taking the first group of parameters in Tab. 2 as an example, the experimental results and simulation results were compared and analyzed under the same conditions. The MF of NCSBMC was simulated in 3D using AdvantEdge finite element simulation software. In the simulation process, in order to reduce the grid division and calculation time, the NCSBMC model was simplified as shown in Fig. 4. After polynomial fitting to obtain MF simulation results. According to the inductive analysis of experimental data and simulation data, by taking the average value and ignoring the influence of the coordinate system setting on the positive and negative values, MF experimental data of NCSBMC is compared with the simulation data as shown in Fig. 5.

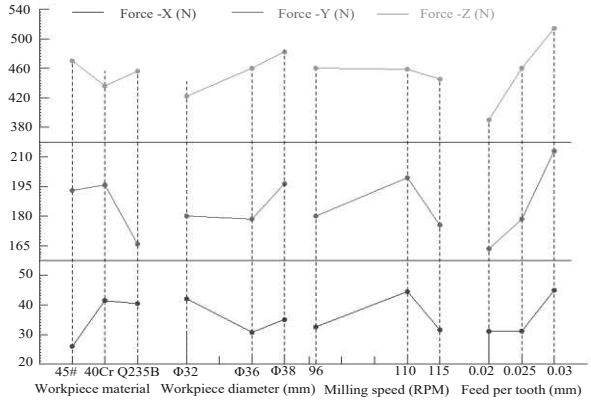

Fig. 3 *Relationship between four factors and three indicators.*

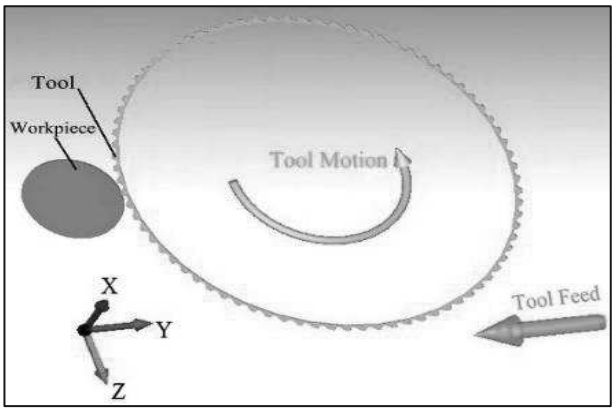

Fig. 4 *MF 3D simulation of NCSBMC*

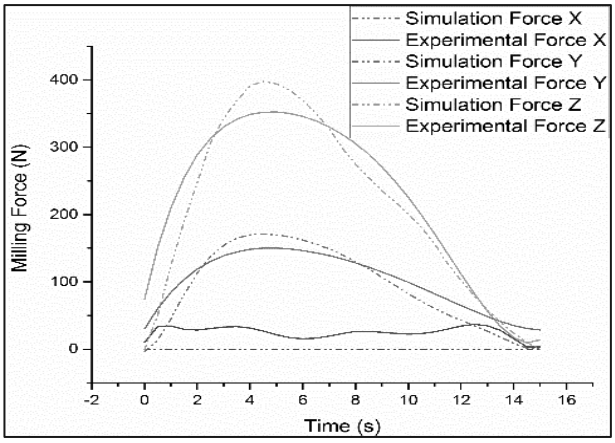

Fig. 5 *Comparison of experimental and simulation values for MF*

Fig. 5 shows that for 45 steel with a diameter of φ32mm, NCSBMC takes about 15 seconds to cut off the workpiece from the entry of the teeth. For F_Y and F_Z, the experimental and simulation curves are generally downward parabolic, and the milling time corresponding to the peak of MF is roughly between the 4th and 8th seconds, when NCSBMC is involved in milling the largest number of teeth and the largest force. For F_X, the experimental values fluctuate in the range of about 20N due to external conditions such as vibration, while the simulation values are almost zero.

The peak of MF obtained from simulation is slightly larger than that obtained from experiment, and the difference of F_Z is slightly obvious, however, by comparing simulation curve of MF with experimental curve, it can be seen that the overall trend of change is close to each other. Compared with simulation data, the accuracy of experimental data is verified, which provides accurate and reliable data for the accurate prediction of MF model.

3 MF model prediction

3.1 Regression analysis

The relationship between the milling parameters and MF can be expressed in the form of an exponential function [19-21]. There are many factors that affect MF, this paper only considers four factors: workpiece material (M), workpiece diameter (D), milling speed (R) and feed per tooth (W). For NCSBMC, the empirical formula for the MF is shown in equation (1).

$$F_i = K_i M^{a_i} D^{b_i} R^{c_i} W^{d_i} \tag{1}$$

Where:

F_i represents MF in i-direction [N],

K_i is i-direction determines the combined correction coefficient factor for milling conditions, friction coefficient, etc.[-],

a_i, b_i, c_i and d_i are the unknowns to be solved [-].

Taking both sides of MF expression in Eq. (1)

$$l\,g\,F_i = \lg K_i + a_i \lg M + b_i \lg D + c_i \lg R + d_i \lg W \tag{2}$$

Suppose $E = lg\ F$, $X_0 = lg\ K$, $X_1 = lg\ M$, $X_2 = lg\ D$, $X_3 = lg\ R$, $X_4 = lg\ W$, we can get Eq. (3)

$$E_i = X_0 + a_i X_1 + b_i X_2 + c_i X_3 + d_i X_4 \tag{3}$$

Using the orthogonal test data in Tab. 2, the test values corresponding to the F_X, F_Y and F_Z were fitted by multiple linear regression analysis with the help of Matlab mathematical calculation software. The corresponding Rockwell hardnesses are used as fitting data for the workpiece materials, and the Rockwell hardness of 45 steel, 40Cr, Q235B is 28HRC, 32HRC, and 15HRC, respectively. In order to eliminate differences between data orders and to reduce errors in data processing, the data in Tab. 2 are normalized to the corresponding values distributed between [0,1]. After fitting the solution to the value of each coefficient in the expression, the empirical formula of F_X, F_Y and F_Z can be obtained as shown in equation (4).

$$\begin{aligned} F_X &= 0.52991 M^{-0.6137} D^{1.4347} R^{-0.3483} W^{-0.540} \\ F_Y &= 4550.9284 M^{0.3818} D^{-0.0476} R^{-0.1934} W^{0.9156} \\ F_Z &= 865.7650 M^{-0.03} D^{0.7491} R^{-0.1523} W^{0.6791} \end{aligned} \tag{4}$$

To verify the accuracy of Eq. (4), on the one hand, the prediction values of MF are compared with the experimental values, as shown in Tab. 4, where $\widehat{F}_X$, $\widehat{F}_Y$ and $\widehat{F}_Z$ represent the predicted values of MF in three axes obtained from Eq. (4). ΔF_X, ΔF_Y, and ΔF_Z represent the deviation values between the predicted MF and the experimental MF in Tab. 2.

$$\begin{aligned} \Delta F_X &= \hat{F}_X - F_X \\ \Delta F_Y &= \hat{F}_Y - F_Y \\ \Delta F_Z &= \hat{F}_Z - F_Z \end{aligned} \tag{5}$$

From Tab. 4, the overall MF predictions are close to the experimental values, with the best prediction accuracy for the F_Y, followed by the F_Z.

On the other hand, the empirical formula is analyzed for the rationality of the residual error. The residual analysis diagram of the F_X, F_Y and F_Z empirical formula of NCSBMC is shown in Fig. 6, where 6(a), 6(b), and 6(c) are the results of F_X, F_Y and F_Z residual analysis, respectively.

As we can see from Fig. 6, the residuals of empirical formula for F_X, F_Y and F_Z are uniformly distributed near the zero line and within the confidence interval, which means that the regression model is in accordance with the original data. The significance test values of F_X, F_Y and F_Z regression equation are 5.3840, 39.9559 and 15.1665 respectively, which are all greater than 0, and meet the requirement of data fit. From the values, the best prediction accuracy of the regression equation for the F_Y is obtained, followed by the F_Z. According to Tab. 4 and Fig. 6, the empirical formula for MF of NCSBMC can be used as a theoretical reference and guide in actual production.

Tab. 4 *Prediction values and deviation values of MF*

	Prediction values of MF(N)			Deviation values of MF(N)		
	$\widehat{F}_X$	$\widehat{F}_Y$	$\widehat{F}_Z$	ΔF_X	ΔF_Y	ΔF_Z
1	16.693	158.500	367.980	-6.889	-3.194	-11.170
2	16.711	188.320	458.090	-7.866	-6.028	-26.690
3	16.114	220.060	536.250	-12.654	-2.798	-11.606
4	11.783	235.490	472.780	-53.328	1.937	5.262
5	17.101	160.170	389.450	-9.430	1.140	21.463
6	17.446	202.930	458.070	-15.565	7.246	-16.028
7	20.382	147.950	424.450	-16.935	3.249	5.343
8	23.291	180.020	539.330	-17.666	-2.068	12.440
9	29.88	120.660	417.690	-13.678	-50.234	-6.673

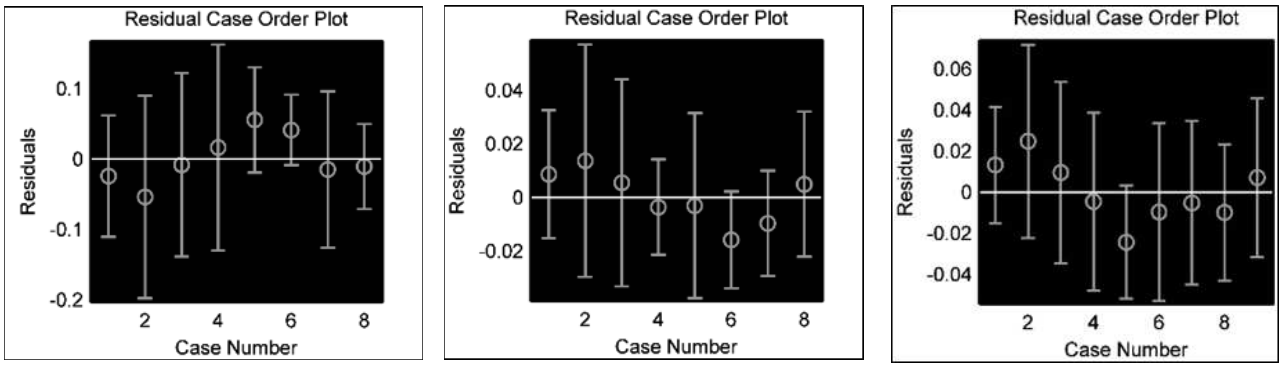

a) *b)* *c)*

Fig. 6 *Residual error analysis diagram of MF empirical formula.*

3.2 DNN MF prediction

A neural network is an extension based on a perceptual machine, while a DNN can be understood as a neural network with many hidden layers. DNN is divided by the location of different layers, neural network layers can be divided into three categories, input, hidden and output layers, and layers are fully connected. The network architecture of DNN in this paper is shown in Fig. 7, which includes an input layer, two hidden layers and an output layer. The input layer is the four characteristic values in Tab. 2. The two hidden layers both contain 64 neurons, and the output layer is the predicted value of F_X, F_Y and F_Z.

Seven groups of data in Tab. 2 were selected as the sample data of the training model, and the remaining two groups were used as the test group to test the model. The MinMaxScaler normalization was performed on the input data, and the learning rate was set to 0.1. We use *Relu* activation as a non-linear activation function, it allows the DNN to introduce sparsity on its own, while greatly improving training speed.

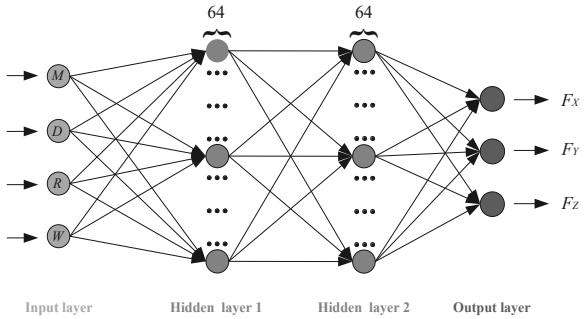

Fig. 7 *Schematic of a DNN structure used in this study*

DNN's forward propagation algorithm uses multiple weighted factor matrices, bias vector to perform a series of linear and activation operations on the input value vector, starting at the input layer and scaling backward layer by layer until it reaches the output layer.

The back propagation (BP) of the DNN is used to calculate the error at each layer of the forward propagation, and the weights and deviations are updated by minimizing the *Loss* function based on the error value.

$$Loss = \frac{1}{2}\sum_{j\in N}\left(d_j - y_j\right)^2 \tag{6}$$

Where:

Loss using mean squared error (MSE) and Mean Absolute Error (MAE) as evaluation indicators [-],

N represents all neurons in the output layer [-],

d_j and y_j are the expected and output values of the *j*-th neuron in the output layer, respectively [-].

In order to prevent over-fitting and excessive learning rate leading to non-convergence, and to speed up the learning process and improve the tuning efficiency, when the degree of *Loss* on the training set is less than a certain threshold, two methods, Early stopping and callback function (ReduceLROnPlateau), are used to stop further training and prevent the accuracy on the test set from decreasing as a result of further training. The change in the number of training sessions and the *Loss* value is shown in Fig. 8.

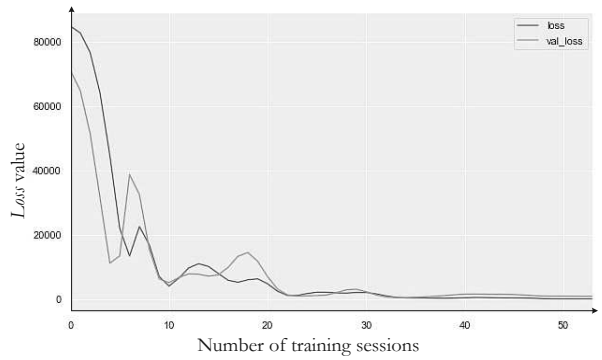

Fig. 8 *Changes in the number of training sessions and Loss value*

In Fig. 8, the horizontal coordinate represents the number of training sessions, the vertical coordinate represents the *Loss* value. The blue line represents the change in the *Loss* value with the number of training sessions on the training set, and the orange line represents the change in the *Loss* value with the number of training sessions on the validation set. As shown in Fig. 8, the *Loss* value converges as the number of training sessions increases.

In DNN model, the data is divided into a training set and a testset. In the case of insufficient data, in order to make full use of the data to test the effect of the algorithm, the data is divided into five groups, one of which is used as a testset at a time, while the remaining four groups are used as a training set. The *K*-fold cross-validation each data has only one chance to be classified into the training or testset during each iteration, the validation and testset alternate with each other to form a complementary set loop, with the result of the model equal to the average of four iterations of MSE and MAE, as shown in Fig. 9.

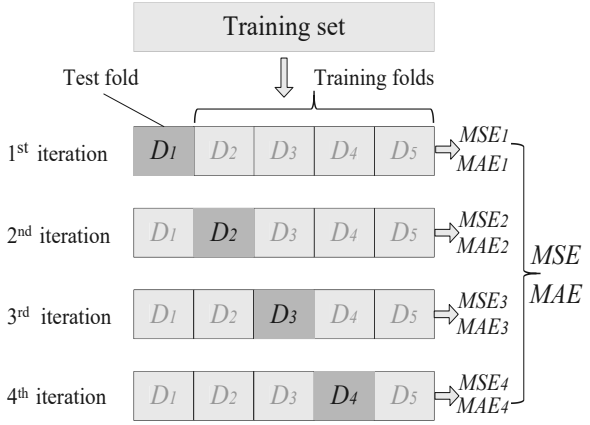

Fig. 9 *Five-fold cross-validation in four iterations*

The results of *K*-fold cross-validation are shown in Tab. 5, for the MSE and MAE, respectively. It can be seen from Tab. 5 that, except for the fluctuations in the MAE and MSE values of the 4th iteration, the MAE and MSE values of the remaining three iterations have relatively small fluctuations.

Tab. 5 *DNN model MF prediction values*

Test fold	MSE	MAE
D_1	259.7263	11.3574
D_2	176.0991	11.3406
D_3	233.6315	11.1843
D_4	931	22.8447

4 Comparison and discussion

The MSE and MAE of MF empirical formula are shown in Eqs. (7) and (8), the MSE and MAE of the DNN MF prediction model are shown in Eqs. (9) and (10), and the r of both MF empirical formula and the DNN MF prediction model are shown in Eq. (11) in combination with the calculations in Tab. 4.

$$MSE = \frac{1}{9}\sum_{i=1}^{9}\left[\left(F_{X_i} - \hat{F}_{X_i}\right)^2 + \left(F_{Y_i} - \hat{F}_{Y_i}\right)^2 + \left(F_{Z_i} - \hat{F}_{Z_i}\right)^2\right] \quad (7)$$

$$MAE = \frac{1}{9}\sum_{i=1}^{9}\left[\left|\left(F_{X_i} - \hat{F}_{X_i}\right)\right| + \left|\left(F_{Y_i} - \hat{F}_{Y_i}\right)\right| + \left|\left(F_{Z_i} - \hat{F}_{Z_i}\right)\right|\right] \quad (8)$$

$$MSE = \frac{1}{4}\sum_{i=1}^{4} MSE_i = \frac{259.73+176.10+233.63+931}{4} = 400.115 \quad (9)$$

$$MAE = \frac{1}{4}\sum_{i=1}^{4} MAE_i = \frac{11.36+11.34+11.18+22.84}{4} = 14.18 \quad (10)$$

$$r = 1 - \frac{\sum_{i=1}^{9}\left[\left(\hat{F}_{X_i} - F_{X_i}\right)^2 + \left(\hat{F}_{Y_i} - F_{Y_i}\right)^2 + \left(\hat{F}_{Z_i} - F_{Z_i}\right)^2\right]}{\sum_{i=1}^{9}\left[\left(\overline{F}_X - F_{X_i}\right)^2 + \left(\overline{F}_Y - F_{Y_i}\right)^2 + \left(\overline{F}_Z - F_{Z_i}\right)^2\right]} \quad (11)$$

Where:

F_{X_i}, F_{Y_i} and F_{Z_i} are milling forces in the three directions of X axis, Y axis and Z axis in Tab. 2, respectively [N],

$\hat{F}_{X_i}$, $\hat{F}_{Y_i}$ and $\hat{F}_{Z_i}$ are the milling forces fitted by the multiple linear regression analysis in the directions of X, Y and Z in Tab. 2 [N], where the value of i ranges from 1 to 9 [-],

$\overline{F}_X$, $\overline{F}_Y$ and $\overline{F}_Z$ are the average values of milling forces in the directions of X, Y, and Z in Tab. 2 [N],

r is the correlation coefficient [-].

Tab. 6 shows the calculation results of MSE, MAE and r values of the MF empirical formula and the DNN MF prediction model. Three performance metrics are analyzed by comparing DNN and regression analysis. It is obvious that DNN far outperformed regression analysis for all the responses.

Tab. 6 *Performance metrics comparison of regression analysis and DNN model*

	MSE	MAE	r
regression analysis	980.616	138.731	0.775
DNN model	400.115	14.18	0.908

5 Conclusion

Experimental research on MF was carried out by means of a four factors and three levels orthogonal test method. According to the results of MF test in this study to predict MF of NCSBMC with regression analysis and DNN model. The findings are summarized as follows:

1) Workpiece diameter, workpiece material, milling speed and feed per tooth all have an impact on MF, with feed per tooth having the greatest impact, followed by workpiece diameter, workpiece material and milling speed.

2) According to experimental research, NCSBMC F_Z range is 300-500N, F_Y range is 150-200N, and F_X range is 20-50N. In actual production, for 20 steel, Q235B and other good processing performance with smaller diameter of low carbon steel workpiece, we can improve the feed per tooth to improve production efficiency. For 40Cr, stainless steel, die steel and other poor processing performance with larger diameter workpiece, in the premise of not affecting the production efficiency, processing parameters should choose smaller feed per tooth and higher speed.

3) A five-fold cross-validation with four iterations is implemented for the DNN model, in order to make full use of the data to test the effect of algorithm in case of insufficient sample size, which effectively avoids the occurrence of over-fitting and under-learning states, and the final fit results are useful for reliable evaluation of the model.

4) The DNN model far outperformed regression analysis for MF prediction for MAE, MSE and r metrics in the absence of sufficient data. The self-learning and adaptive capabilities of DNN makes the prediction accuracy higher than that of empirical formulas. Compared with the empirical formula of linear regression analysis, the DNN has better scalability. The empirical formula fitted by the linear regression analysis needs to presuppose an exponential relationship between MF and the machining parameters, while DNN is more capable of modeling and processing non-linear models.

Acknowledgments

This research was financially supported by the National International Scientific and Technological Cooperation Special with Granted No.2018DFR50520 and by Fujian Provincial Key Project of Science and Technology with Granted No. 2019H0034.

References

[1] CHANG W T., CHEN L C. (2016). Design and experimental evaluation of a circular saw blade

with self-clamped cutting inserts. In: *International Journal of Advanced Manufacturing Technology*, Vol. 83, No. 1-4, pp. 365-379. ISSN 0268-3768.

[2] GUO J F. (2005). The application of metal cold cutting circular saw blade in steel rolling production. In: *Metallurgical Equipment*, Vol. 6, No. 1, pp. 43-48. ISSN 1001-1269.

[3] GUO S L., GU L Z., HAN J X., ZHONG C. (2018). Parameter comparison and performance analysis of new cold saw blade milling cutter and traditional saw blade milling cutter. In: *Tool Technology*, Vol. 52, No. 3, pp. 71-76. ISSN 1000-7008.

[4] YADAV R K., ABHISHEK K., MAHAPATRA S S. (2015). A simulation approach for estimating flank wear and material removal rate in turning of Inconel 718. In: *Simulation Modelling Practice and Theory*, Vol. 52, No. 1, pp. 1-14. ISSN 1569-190X.

[5] SHAN G., PENG N. (2012). Application of Improved L-M Optimization Algorithm BP Neural Network in Tool Wear Prediction. In: *Machine Tool and Hydraulics*, Vol. 40, No. 15, pp. 22-26. ISSN 1001-3881.

[6] XU Z H., LI S., CHEN Q W. (2015). Consistency tracking control of multiple Euler-Lagrange systems using velocity observers. In: *Control Theory and Applications*, Vol. 32, No. 1, pp. 50-57. ISSN 1000-8152.

[7] S. CAMPOCASSO et al. (2017). Towards cutting force evaluation without cutting tests. In: *CIRP Annals*, Vol. 66, No. 1, pp. 77-80. ISSN 0007-8506.

[8] JÁNOS KUNDRÁK et al. (2018). Analysis of the Effect of Feed on Chip Size Ratio and Cutting Forces in Face Milling for Various Cutting Speeds. In: *Manufacturing Technology*, Vol. 18, No. 3, pp. 431-438. ISSN 1213-2489.

[9] GENG G S et al. (2020). Finite Element Analysis and Parameter Optimization Selection of High Speed Milling GH4169. In: *Manufacturing Technology*, Vol. 20, No. 3, pp. 300-306. ISSN 1213-2489.

[10] LI Y., XU X P. (2005). Finite Element Analysis of Saw Blade Force in Large Cutting Depth Cutting Stone. In: *Chinese Journal of Engineering Machinery*, Vol. 6, No. 3, pp. 267-271. ISSN 1672-5581.

[11] HU C G., ZHANG D H., RENG J X., YANG L. (2006). Summary of Cutting Force Modeling Methods. In: *Progress in Mechanics*, Vol. 4, No. 4, pp. 564-570. ISSN 1000-0992.

[12] TANG J Y., LIN X J., TANG J J., LOU J L. (2012). Force-energy simulation study of metal sawing process based on DEFORM-3D. In: *Manufacturing Technology and Machine Tools*, Vol. 12, No. 8, pp. 99-103. ISSN 1005-2402.

[13] ZHU K P., ZHANG Y. (2017). Modeling of the instantaneous milling force per tooth with tool run-out effect in high speed ball-end milling. In: *International Journal of Machine Tools and Manufacture*, Vol. 118-119, pp. 37-48. ISSN 0890-6955.

[14] S. TURCHETTA., L. SORRENTINO. (2019). Forces and wear in high-speed machining of granite by circular sawing. In: *Diamond and Related Materials*, Vol. 100, ISSN 0925-9635.

[15] KAIS I. ABDUL-LATEEF AL-ABDULLAH et al. (2018). Force and temperature modelling of bone milling using artificial neural networks. In: *Measurement*, Vol. 116, pp. 25-37. ISSN 0263-2241.

[16] LI X., SHI Z Y et al. (2018). Artificial neural network predicts tool wear and cutting force. In: *Control Theory and Applications*, Vol. 35, No. 12, pp. 1731-1737. ISSN 1000-8152.

[17] WANG J C et al. (2020). Milling force prediction model based on transfer learning and neural network. In: *Journal of Intelligent Manufacturing*, pp. 1-10. ISSN 0956-5515.

[18] ALI YEGANEFAR et al. (2019). The use of support vector machine, neural network, and regression analysis to predict and optimize surface roughness and cutting forces in milling. In: *International Journal of Advanced Manufacturing Technology*, Vol. 105, No. 2, pp. 951-965. ISSN 1672-5581.

[19] HAN X., LIU Q. (2010). Modeling and analysis of PH13-8Mo plunge milling force. In: *Aviation Manufacturing Technology*, Vol. 24, No. 5, pp. 72-80. ISSN 1671-833X.

[20] ZHU L., LU D N. (2018). Design of CNC constant force milling tool path. In: *Machine Tool and Hydraulics*, Vol. 46, No. 8, pp. 9-12. ISSN 1001-3881.

[21] SUN J J, KONG X etc. (2011). Experimental research on the milling force model of 6061 aluminum alloy ball end milling cutter. In: *Tool Technology*, Vol. 45, No. 1, pp. 22-25. ISSN 1000-7008.